

Bottomonia production in p+p collisions under NRQCD formalism

Vineet Kumar^{a,*}, Kinkar Saha^b, Prashant Shukla^{a,c}, Abhijit Bhattacharyya^b

^a*Nuclear Physics Division, Bhabha Atomic Research Centre, Mumbai 400085, India*

^b*Department of Physics, University of Calcutta, 92, A. P. C. Road Kolkata-700009, India*

^c*Homi Bhabha National Institute, Anushakti Nagar, Mumbai 400094, India*

Abstract

In this work, we present the calculation of the production cross sections of bottomonia states using Non-Relativistic Quantum Chromodynamics (NRQCD) formalism. The direct production cross-section of a resonance can be factorised in terms of short distance Quantum Chromodynamics (QCD) cross sections and long distance matrix elements (LDMEs) under NRQCD. We use a large set of measured $\Upsilon(nS)$ production data at Tevatron and LHC energies in both central and forward rapidity regions to extract the LDMEs with better precision. The feed down contributions from the higher states including the $\chi_b(3P)$ state are taken into account for the LDME extraction. The formalism provides a good description of the bottomonia data in wide transverse momentum range at different collision energies.

Keywords: Quarkonia, NRQCD

1. Introduction

Quantum Chromodynamics (QCD) describes the strong interaction among the quarks and gluons via perturbative calculations utilising its property called asymptotic freedom. On the other hand, these quarks and gluons are confined inside hadrons which are the colour singlet states. Confinement is a purely non-perturbative phenomenon which is not very well understood yet. The study of quarkonia ($Q\bar{Q}$) serves as an effective tool to look at both of these perturbative and non-perturbative aspects of QCD. The quarkonia states differ from most other hadrons due to the small velocity, v of the massive constituents and thus can be treated using non-relativistic formalism [1, 2]. In a simple picture, one can think of a quarkonium as a heavy quark pair ($Q\bar{Q}$) bound in a colour singlet state by some effective potential interaction, where the constituents are separated by distances much smaller than $1/\Lambda_{\text{QCD}}$ where Λ_{QCD} is the QCD scale. This interaction gets screened in the presence of a deconfined medium like Quark Gluon Plasma (QGP), causing the bound state to melt away and thus the quarkonia yields are suppressed in the heavy ion collisions. This makes quarkonia an important probe of QGP. However cold nuclear matter effects such as modification of parton distribution functions of nucleons inside nucleus also affect their yields. There have been immense experimental [3, 4, 5, 6] and theoretical works [7, 8, 9, 10] on quarkonia modifications in PbPb collisions for which understanding of quarkonia production in pp collisions is an important prerequisite.

*Corresponding author

Email address: vineetk@barc.gov.in (Vineet Kumar)

The massive quarks (with $m_c \sim 1.6 \text{ GeV}/c^2$, $m_b \sim 4.5 \text{ GeV}/c^2$) are produced in initial stages in hadronic collision with high momentum transfer and thus can be treated perturbatively [11]. The emergence of quarkonia out of the two massive quarks, on the other hand can only be described non-perturbatively using different models [12, 13]. The Colour Singlet Model (CSM) [14, 15], Colour Evaporation Model (CEM) [16, 17], the Fragmentation Scheme and the NRQCD factorisation formalism are some of the well established models for quarkonia production. In the framework of CSM, the $Q\bar{Q}$ pair, eventually evolving into the quarkonium, is assumed to be in Colour Singlet (CS) state and that has spin and angular momentum same as that of quarkonium. Apart from comprising of the CSM, the NRQCD factorisation approach incorporates the Colour Octet (CO) states as well.

In the formalism of the NRQCD factorisation approach, the evolution probability of $Q\bar{Q}$ pair into a state of quarkonium is expressed as matrix elements of NRQCD operators expanded in terms of heavy quark velocity v (for $v \ll 1$) [12]. The factorisation formulae were then used to calculate production cross-sections and decay rates of quarkonia states. The full structure of the $Q\bar{Q}$ Fock space is considered and spanned by $n=2s+1 L_J^{[a]}$ state where s is the spin, L is the orbital angular momentum, J is the total angular momentum and a (colour multiplicity) = 1 for CS and 8 for CO states. The produced CO states of $Q\bar{Q}$ pair at short distances emerge as CS quarkonia by emitting soft gluons non-perturbatively. The short distance cross-sections are obtained theoretically using methods of perturbative QCD (pQCD). The long distance matrix elements (LDME) that correspond to the probability of $Q\bar{Q}$ pair to emerge as quarkonium are extracted by fitting the measured cross-section data.

There have been several works on bottomonia production based on NRQCD formalism. In Ref. [18], a Monte Carlo framework has first been employed with CO mechanism for inclusive bottomonia production and few NRQCD CO matrix elements for $\Upsilon(1S)$ have been extracted at the Tevatron energy. The study has been extended to the whole $\Upsilon(nS)$ family in Ref. [19] to find CO matrix elements using CDF measurements at Tevatron. In Ref. [20] the CO matrix elements are obtained for $\Upsilon(nS)$ family and the feed downs from $\chi_b(1P)$ and $\chi_b(2P)$ to $\Upsilon(1S)$ have been considered. In Ref. [21], the Υ production has been obtained via S-wave CO states calculated at Next to Leading Order (NLO). The LDMEs are obtained by fitting the Tevatron data. The ratios of NLO to LO total cross-sections have been obtained at Tevatron and LHC energies. Polarisation of inclusive Υ has been obtained albeit with large uncertainties. In Ref. [22] both CS and CO states along with feed down contributions from higher states have been considered to study the quarkonia yields for RHIC and LHC energies. Using Collins-Soper-Sterman (CSS) formalism, an extension of the NRQCD prediction has been carried forward for heavy quarkonium production at low p_T by considering soft gluon resummation at all orders in Ref. [23].

Both production and polarisation of $\Upsilon(nS)$ at NLO have been discussed in Ref. [24] within the framework of NRQCD. The CO matrix elements are obtained by fitting with experimental data. The study is updated in Ref. [25] by considering feed down from $\chi_{bJ}(mP)$ states in $\Upsilon(nS)$ production. The yields and polarisations of $\Upsilon(nS)$ measured at Tevatron and LHC are well explained by this work. The NLO study in Ref. [26] describes the yields and polarisations of $\Upsilon(nS)$ at LHC which includes feed down contributions from higher states. Ref. [27] gives complete analysis of the polarization parameters of $\Upsilon(nS)$ at QCD next-to-leading

order in both the helicity and Collins-Soper frames. In Ref. [28], production cross-section for $\Upsilon(nS)$, χ_{bJ} , η_b and h_b have been calculated using NRQCD, as produced in hard photo production and fragmentation processes at LHC energies.

A LO NRQCD analysis is useful as it is straightforward and unique and once the parameters are obtained by fitting over large datasets it has excellent predictability power for unknown cross sections. The short distance QCD cross-sections calculation techniques at NLO are not unique. Moreover the different components of pQCD NLO cross sections are not available in public domain. Many NLO analysis do not include the feed down contribution from the higher states. It is shown that there is a large difference among the LDMEs obtained by different analysis at NLO. In this paper, the LO NRQCD calculations for the differential production cross-sections of Υ states in p+p collisions have been presented. Our work includes most up to date datasets and feeddown contributions. We have given an estimate of uncertainties in the LDMEs due to enhancement of CS quarkonia cross-section by a factor of two expected from the NLO corrections, only slight changes appear in the CO quarkonia cross-section when the NLO QCD corrections are included [21, 29].

The NRQCD formalism is described briefly in Section 2. A large set of data from Tevatron [30] and LHC [31, 32, 33, 34, 35] is used to extract the LDMEs required for the Υ production and then results are presented in Section 3. A comparison of the obtained LDMEs with the previous NRQCD studies both at LO and NLO has been made. The summary of our findings are discussed in Section 4.

2. Bottomonia production in p+p collisions

In order to study heavy quarkonium yield, the NRQCD framework serves as an efficient theoretical tool. The processes that govern the differential production of heavy mesons like bottomonium, as functions of p_T are mostly $2 \rightarrow 2$ operations. These processes can be denoted generically by $a + b \rightarrow \Upsilon + X$, where a and b are the incident light partons, Υ is the heavy meson and X is final state light parton. The double differential cross-section as a function of p_T and rapidity (y) of the heavy meson can be written as [36],

$$\begin{aligned} \frac{d^2\sigma^\Upsilon}{dp_T dy} &= \sum_{a,b} \int_{x_a^{min}}^1 dx_a G_{a/p}(x_a, \mu_F^2) G_{b/p}(x_b, \mu_F^2) \\ &\times 2p_T \frac{x_a x_b}{x_a - \frac{m_T}{\sqrt{s}} e^y} \frac{d\sigma}{d\hat{t}} \end{aligned} \quad (1)$$

where, $G_{a/p}(G_{b/p})$ are the colliding parton ($a(b)$) distribution functions in the incident protons. They depend on the fractions $x_a(x_b)$, of the total momentum carried by the incident partons and the scale of factorisation μ_F . Here \sqrt{s} represents the total center of mass energy of the pp system and $m_T (= \mu_F)$ stands for the transverse mass, $m_T^2 = p_T^2 + M^2$ of the quarkonium. The one loop $\alpha_s(Q^2)$ is used in the calculations and value of the Q^2 is taken equal to the square of the scale of factorisation (μ_F). The relation between x_a and x_b and the expression for x_a^{min} are given in our earlier work [36]. The $d\sigma/d\hat{t}$ in Eq. 1 is the parton level cross-section and is defined as [12],

$$\frac{d\sigma}{d\hat{t}} = \frac{d\sigma}{d\hat{t}}(ab \rightarrow Q\bar{Q}(^{2s+1}L_J) + X) M_L(Q\bar{Q}(^{2s+1}L_J) \rightarrow \Upsilon) \quad (2)$$

Table 1: Necessary and pertinent branching fractions for bottomonia family [26, 42].

Meson from	Meson to								
	$\Upsilon(3S)$	$\chi_{b0}(2P)$	$\chi_{b1}(2P)$	$\chi_{b2}(2P)$	$\Upsilon(2S)$	$\chi_{b0}(1P)$	$\chi_{b1}(1P)$	$\chi_{b2}(1P)$	$\Upsilon(1S)$
$\chi_{b0}(3P)$	0.005				0.002				0.002
$\chi_{b1}(3P)$	0.104				0.037				0.038
$\chi_{b2}(3P)$	0.061				0.019				0.019
$\Upsilon(3S)$		0.131	0.126	0.059	0.199	0.003	0.0017	0.019	0.066
$\chi_{b0}(2P)$					0.014				0.004
$\chi_{b1}(2P)$					0.199				0.092
$\chi_{b2}(2P)$					0.106				0.070
$\Upsilon(2S)$						0.038	0.0715	0.069	0.260
$\chi_{b0}(1P)$									0.019
$\chi_{b1}(1P)$									0.352
$\chi_{b2}(1P)$									0.180

Table 2: CS and CO elements for Υ family, obtained theoretically/extracted using experimental data [22, 25].

Direct Contributions	Feed down contributions from higher s-wave states	Feed down contributions from higher p-wave states
$M_L(b\bar{b}([{}^3S_1]_1) \rightarrow \Upsilon(3S))$ $=4.3 \text{ GeV}^3$	$M_L(b\bar{b}([{}^3S_1]_1) \rightarrow \Upsilon(3S, 2S))$ $=4.3, 4.5 \text{ GeV}^3$	$M_L(b\bar{b}([{}^3P_0]_1) \rightarrow \chi_{b0}(1P))$ $=0.100m_b^2 \text{ GeV}^3$
$M_L(b\bar{b}([{}^3S_1]_1) \rightarrow \Upsilon(2S))$ $=4.5 \text{ GeV}^3$	$M_L(b\bar{b}([{}^3S_1]_8) \rightarrow \Upsilon(3S, 2S))$	$M_L(b\bar{b}([{}^3S_1]_8) \rightarrow \chi_{b0}(1P))$ $=0.0094 \text{ GeV}^3$
$M_L(b\bar{b}([{}^3S_1]_1) \rightarrow \Upsilon(1S))$ $=10.9 \text{ GeV}^3$	$M_L(b\bar{b}([{}^1S_0]_8) \rightarrow \Upsilon(3S, 2S))$	$M_L(b\bar{b}([{}^3P_0]_1) \rightarrow \chi_{b0}(2P))$ $=0.100m_b^2 \text{ GeV}^3$
$M_L(b\bar{b}([{}^3S_1]_8) \rightarrow \Upsilon(nS))$	$M_L(b\bar{b}([{}^3P_0]_8) \rightarrow \Upsilon(3S, 2S))$	$M_L(b\bar{b}([{}^3S_1]_8) \rightarrow \chi_{b0}(2P))$ $=0.0109 \text{ GeV}^3$
$M_L(b\bar{b}([{}^1S_0]_8) \rightarrow \Upsilon(nS))$	$M_L(b\bar{b}([{}^3P_1]_8) \rightarrow \Upsilon(3S, 2S))$ $=3M_L(b\bar{b}([{}^3P_0]_8) \rightarrow \Upsilon(3S, 2S))$	$M_L(b\bar{b}([{}^3P_0]_1) \rightarrow \chi_{b0}(3P))$ $=0.100m_b^2 \text{ GeV}^3$
$M_L(b\bar{b}([{}^3P_0]_8) \rightarrow \Upsilon(nS))$	$M_L(b\bar{b}([{}^3P_2]_8) \rightarrow \Upsilon(3S, 2S))$ $=5M_L(b\bar{b}([{}^3P_0]_8) \rightarrow \Upsilon(3S, 2S))$	$M_L(b\bar{b}([{}^3S_1]_8) \rightarrow \chi_{b0}(3P))$ $=0.0069 \text{ GeV}^3$
$M_L(b\bar{b}([{}^3P_1]_8) \rightarrow \Upsilon(nS))$ $3M_L(b\bar{b}([{}^3P_0]_8) \rightarrow \Upsilon(nS))$		
$M_L(b\bar{b}([{}^3P_2]_8) \rightarrow \Upsilon(nS))$ $5M_L(b\bar{b}([{}^3P_0]_8) \rightarrow \Upsilon(nS))$		

The first term in RHS is the short distance contribution, that corresponds to the $Q\bar{Q}$ pair production in specific colour and spin configuration and is calculable using perturbative QCD (pQCD) [20, 37, 38, 39, 40, 41]. The other term in the RHS of Eq.(2) is the Long Distance Matrix Element (LDME) and refers to the probability of the $Q\bar{Q}$ state to convert into a quarkonium state. They are determined by contrasting with experimental observations.

The NRQCD formalism provides an adequate procedure to estimate a quantity as an expansion in heavy quark relative velocity, v inside $Q\bar{Q}$ bound state. The LDME in Eq.(2) do scale with definitive power in v . The quarkonium yield depends on the $^3S_1^{[1]}$ and $^3P_J^{[1]}$ ($J=0,1,2$) CS states and $^1S_0^{[8]}$, $^3S_1^{[8]}$ and $^3P_J^{[8]}$ CO states in the limit $v \ll 1$. The superscripts in square brackets represent the colour structure of the bound state, 1 for the CS and 8 for the CO. The direct production cross-section for Υ in differential form can thus be expressed as the sum of all contributions,

$$\begin{aligned}
d\sigma(\Upsilon(nS)) = & d\sigma(Q\bar{Q}([^3S_1]_1))M_L(Q\bar{Q}([^3S_1]_1) \rightarrow \Upsilon(nS)) \\
& + d\sigma(Q\bar{Q}([^1S_0]_8))M_L(Q\bar{Q}([^1S_0]_8) \rightarrow \Upsilon(nS)) \\
& + d\sigma(Q\bar{Q}([^3S_1]_8))M_L(Q\bar{Q}([^3S_1]_8) \rightarrow \Upsilon(nS)) \\
& + d\sigma(Q\bar{Q}([^3P_0]_8))M_L(Q\bar{Q}([^3P_0]_8) \rightarrow \Upsilon(nS)) \\
& + d\sigma(Q\bar{Q}([^3P_1]_8))M_L(Q\bar{Q}([^3P_1]_8) \rightarrow \Upsilon(nS)) \\
& + d\sigma(Q\bar{Q}([^3P_2]_8))M_L(Q\bar{Q}([^3P_2]_8) \rightarrow \Upsilon(nS)) \\
& + \dots
\end{aligned} \tag{3}$$

The dots include terms having contributions in higher powers of v .

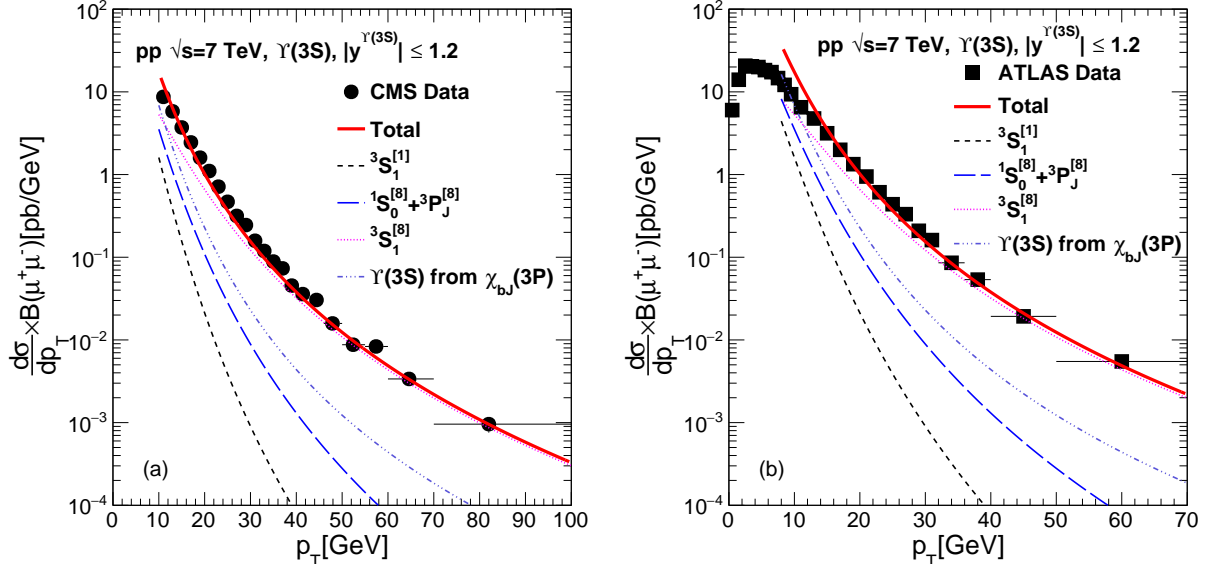


Figure 1: The NRQCD calculations of production cross-section of $\Upsilon(3S)$ in p+p collisions at $\sqrt{s} = 7$ TeV in central rapidities, as a function of transverse momentum compared with the measured data at CMS [32] and ATLAS [33] experiment.

The contributions from CS- $[^3P_J]_1$ and CO- $[^3S_1]_8$ states are in the same order of v for the p-wave bound

states, $\chi_b(nP)$. The angular momentum barriers of the p-wave states are held responsible for that to happen and thereby making them important enough to be considered. The differential cross-section for χ_b production henceforth is given by,

$$\begin{aligned}
d\sigma(\chi_{bJ}(1P)) &= d\sigma(Q\bar{Q}([{}^3P_J]_1))M_L(Q\bar{Q}([{}^3P_J]_1) \rightarrow \chi_{bJ}(1P)) \\
&+ d\sigma(Q\bar{Q}([{}^3S_1]_8))M_L(Q\bar{Q}([{}^3S_1]_8) \rightarrow \chi_{bJ}(1P)) \\
&+ \dots
\end{aligned} \tag{4}$$

The experimental observations of Υ production at LHC energies, not only have contributions from direct yield, but also consist of feed downs from decay of heavier bottomonia states. The corresponding branching fractions are provided in Table 1.

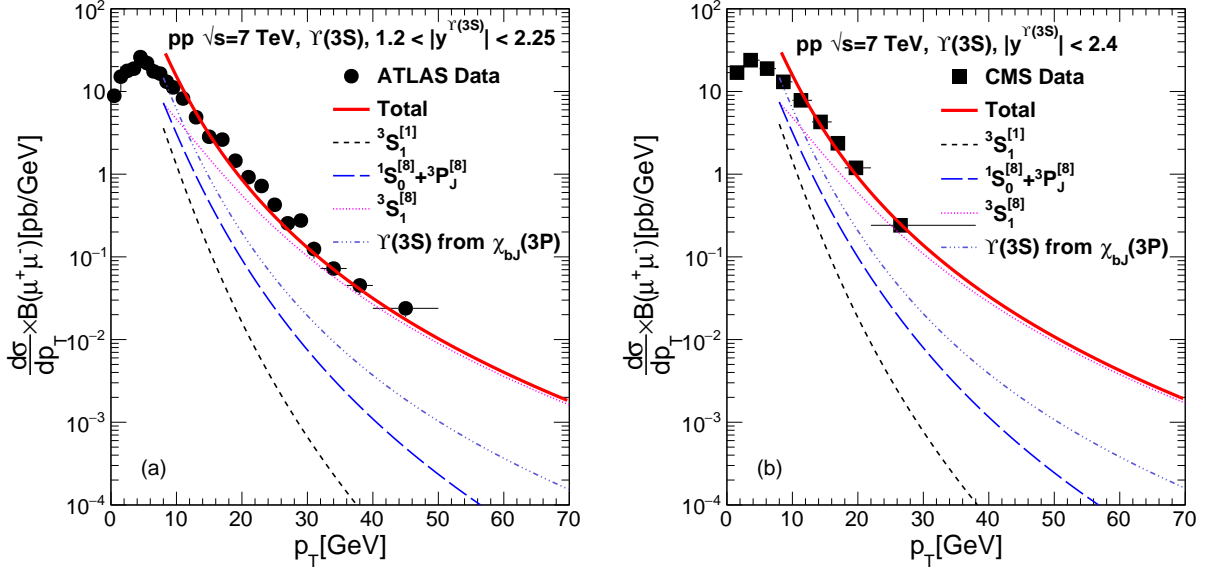


Figure 2: The NRQCD calculations of production cross-section of $\Upsilon(3S)$ in p+p collisions at $\sqrt{s} = 7$ TeV in forward rapidities, as a function of transverse momentum compared with the measured data at ATLAS [33] and CMS [34] experiments.

We require both CS and CO matrix elements in order to get theoretical predictions for the production of bottomonia at the Tevatron and LHC energies. The corresponding expressions and numerical values for CS states are obtained from Ref. [20]. The CO states, on the other hand, cannot be directly connected to the non-relativistic wavefunctions of heavy mesons, as these are associated with a higher Fock state. Experimentally measured data sets are therefore employed to obtain them as in Refs. [20, 40, 41]. The CS operators along with their theoretical values and the CO operators to be fitted are listed in Table 2, where, $n=1,2,3$. For the CO elements related to p-wave states, needed as the feed down contributions, we have used values obtained by Ref. [22, 25] for the present purpose. In our calculations, we have used CT14LO parametrisation [43] for parton distribution functions and the bottom quark mass m_b is taken to be 4.88 GeV. The short distance cross-sections for $[{}^1S_0]_8$ and $[{}^3P_J]_8$ states having similar p_T dependencies, the corresponding distributions become sensitive upto a linear combination of their LDMEs. We therefore take

Table 3: Comparison of CS elements and CO LDMEs extracted from fitting with experimental data using NRQCD formalism for $\Upsilon(3S)$.

Ref. (LO/NLO)	PDF	m_b (GeV)	$M_L(b\bar{b}([{}^3S_1]_1 \rightarrow \Upsilon(3S))$ (GeV ³)	$M_L(b\bar{b}([{}^3S_1]_8 \rightarrow \Upsilon(3S))$ (GeV ³)	$M_L(b\bar{b}([{}^1S_0]_8, [{}^3P_0]_8 \rightarrow \Upsilon(3S))$ (GeV ³)	p_T -cut GeV/ c
present (LO)	CT14LO	4.88	4.3	$0.0547 \pm 0.0007 \pm 0.0036$	$0.0054 \pm 0.0005 \pm 0.0021$	8
[19] (LO)	CTEQ4L	4.88	3.54	0.099 ± 0.011	0	2
				0.091 ± 0.015	0	4
				0.068 ± 0.011	0	8
[20] (LO)	CTEQ5L	4.77	4.3 ± 0.9	0.036 ± 0.019	0.0108 ± 0.0086	8
				0.039 ± 0.017	0.0342 ± 0.0276	
	MRSTLO	4.77	4.3 ± 0.9	0.037 ± 0.021 0.041 ± 0.019	0.0150 ± 0.0098 0.0474 ± 0.0312	8
[21] (NLO)	CTEQ6M	5.18	1.128	0.03250 ± 0.00876	0.000920 ± 0.000968	-
[22] (LO)	MSTW08LO	4.88	4.3	0.0513 ± 0.0085	0.0002 ± 0.0062	-
[24] (NLO)	CTEQ6M	5.18	1.128	0.0271 ± 0.0013	0.00956 ± 0.00476	8
[25] (NLO)	CTEQ6M	5.18	1.128	0.0132 ± 0.0020	-0.00520 ± 0.00518	8

resort to a linear combination following Ref. [36] as,

$$M_L(b\bar{b}([{}^1S_0]_8, [{}^3P_0]_8) \rightarrow \Upsilon(nS)) = \frac{M_L(b\bar{b}([{}^1S_0]_8) \rightarrow \Upsilon(nS))}{5} + \frac{3M_L(b\bar{b}([{}^3P_0]_8) \rightarrow \Upsilon(nS))}{m_b^2}.$$

3. Results and discussions

We first start with the production of $\Upsilon(3S)$ which has feed down contributions only from $\chi_b(3P)$. As described, the expressions and the values for the colour-singlet elements can be obtained by solving the non-relativistic wavefunctions [40]. The CO LDMEs on the other hand, cannot be connected to the non-relativistic wavefunctions of $b\bar{b}$. The measured data sets from different experimental collaborations are thus used to constrain them.

Figure 1 shows the NRQCD calculations of production cross-section of $\Upsilon(3S)$ in p+p collisions as a function of transverse momentum compared with the measured data in CMS [32] and ATLAS [33] detectors at LHC in central rapidities. Figure 1 and all subsequent figures are normalized by corresponding rapidity

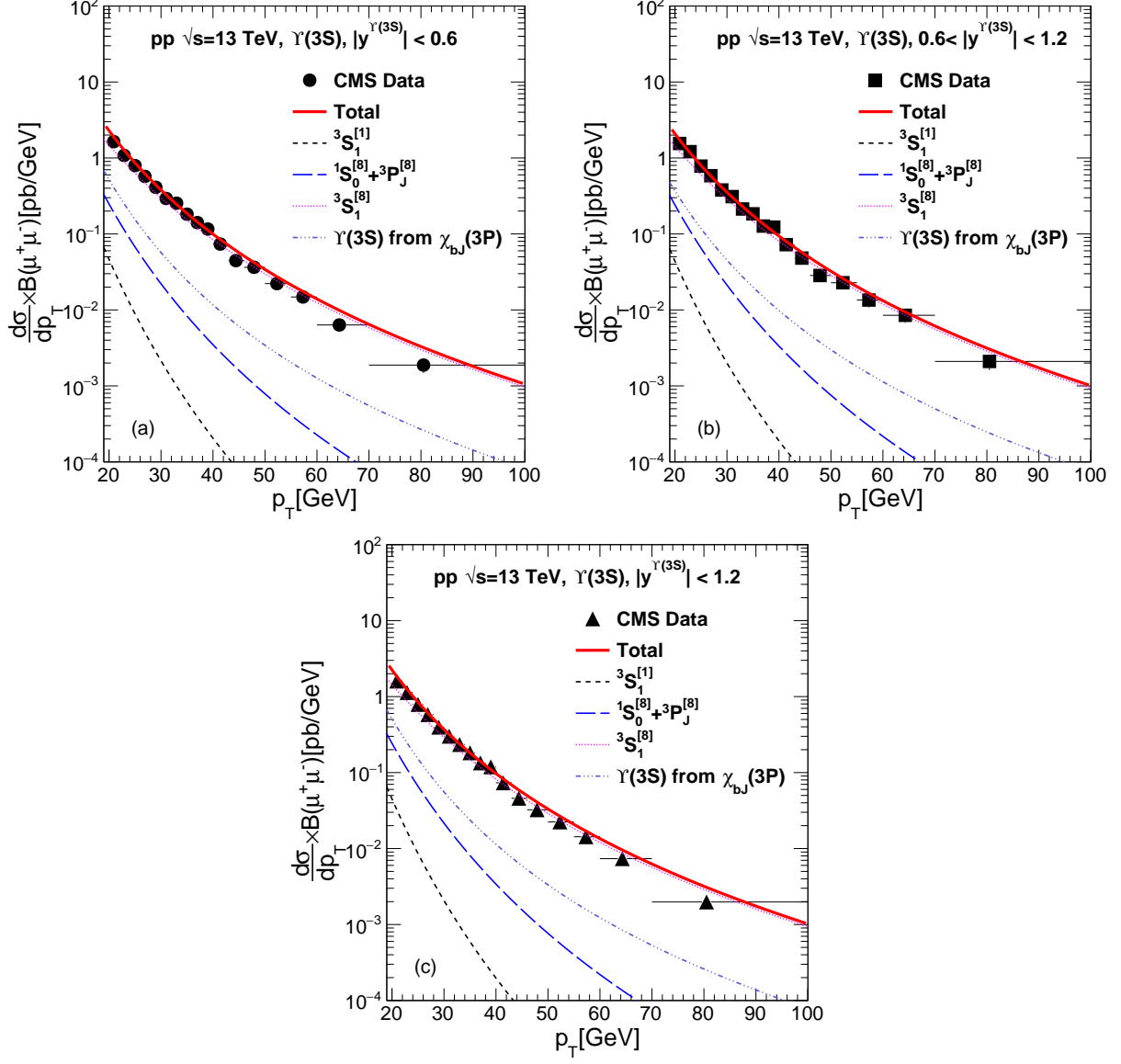


Figure 3: The NRQCD calculations of production cross-section of $\Upsilon(3S)$ in p+p collisions at $\sqrt{s} = 13$ TeV in central and forward rapidities, as a function of transverse momentum compared with the measured data at CMS [35] experiment.

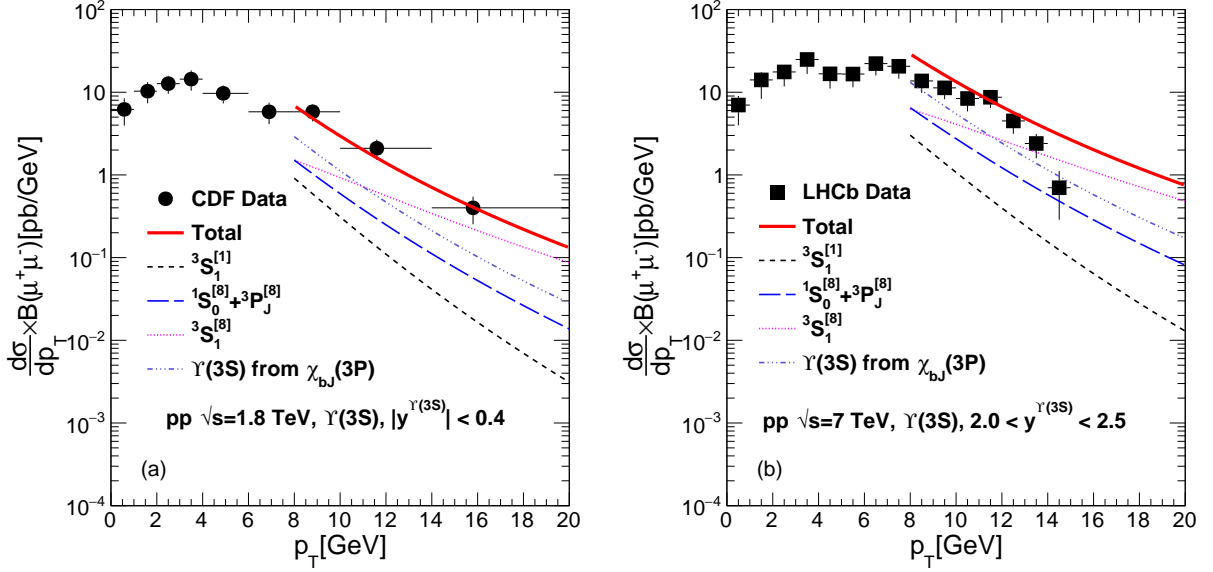


Figure 4: The NRQCD calculations of production cross-section of $\Upsilon(3S)$ in $p + \bar{p}$ collisions at $\sqrt{s} = 1.8$ TeV and $p+p$ collisions at 7 TeV in forward rapidities, as a function of transverse momentum compared with the measured data at CDF [30] and LHCb [31] experiment.

intervals. In Figure 2, similar comparisons have been shown with data for $1.2 < |y| < 2.25$ and $|y| < 2.4$ measured at ATLAS [33] and CMS [34] detectors respectively. Figure 3 corresponds to CMS [35] measurements at $\sqrt{s} = 13$ TeV for rapidities, $|y| < 0.6$, $0.6 < |y| < 1.2$ and $|y| < 1.2$, whereas in Figure 4 we have used measurements from CDF [30] collaboration in $p + \bar{p}$ at $\sqrt{s} = 1.8$ TeV with $|y| < 0.4$ as well as that from LHCb [31] collaboration in $p+p$ collisions at $\sqrt{s} = 7$ TeV with rapidities $2.0 < y < 2.5$. The LDMEs are obtained by a combined fit using all the aforesaid datasets. The χ^2/ndof is ~ 4 for the combined fitting. To estimate the uncertainty in the LDMEs following study is performed by varying two parameters of the calculation

- i We extracted an estimate of uncertainties in the LDMEs due to enhancement of color singlet cross-section of quarkonia by around a factor of two expected from NLO corrections [21, 29].
- ii We changed the mass of the bottom quark to 4.77 GeV from 4.88 GeV and recalculated the short distance cross-sections. LDMEs are then extracted using these cross-sections. This value of the mass is motivated by the use of several groups earlier in their calculations [20, 24].

Both of these uncertainties are then added in quadrature and quoted with the LDME values. Table 3 contains LDMEs for $\Upsilon(3S)$ extracted in present analysis in comparison with different other results. Here the first error is due to the fitting and the second error is obtained by the uncertainty study. Our result for the matrix element $M_L(b\bar{b}([{}^3S_1]_8))$ shows a close proximity with LO analysis of Ref. [20, 22]. In our work, we have considered a linear combination of the other two colour octet LDMEs in the form of $\frac{M_L([{}^1S_0]_8)}{5} + \frac{3M_L([{}^3P_0]_8)}{m_b^2}$, same as that done in Ref. [22]. There have been different ways to treat the colour octet LDMEs in the literature. In Ref. [19], the authors have taken this combination as $M_L([{}^1S_0]_8) + \frac{5M_L([{}^3P_0]_8)}{m_b^2}$. In Ref. [20], these two matrix elements, $M_L([{}^1S_0]_8)$ and $\frac{5M_L([{}^3P_0]_8)}{m_b^2}$ have been extracted separately using two different

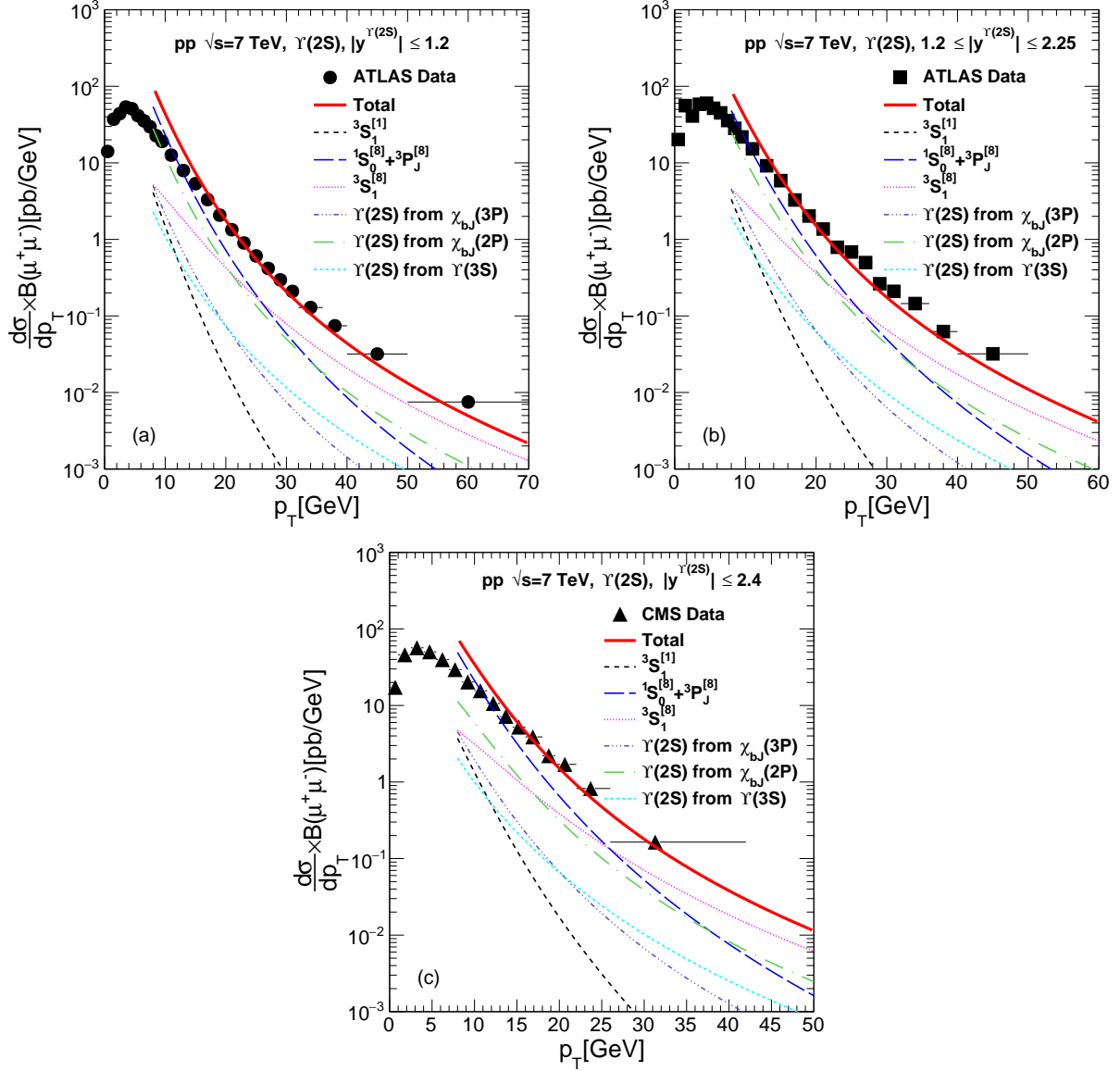


Figure 5: The NRQCD calculations of production cross-section of $\Upsilon(2S)$ in p+p collisions at $\sqrt{s} = 7$ TeV in central and forward rapidities, as a function of transverse momentum compared with the measured data at CMS [34] and ATLAS [33] experiments.

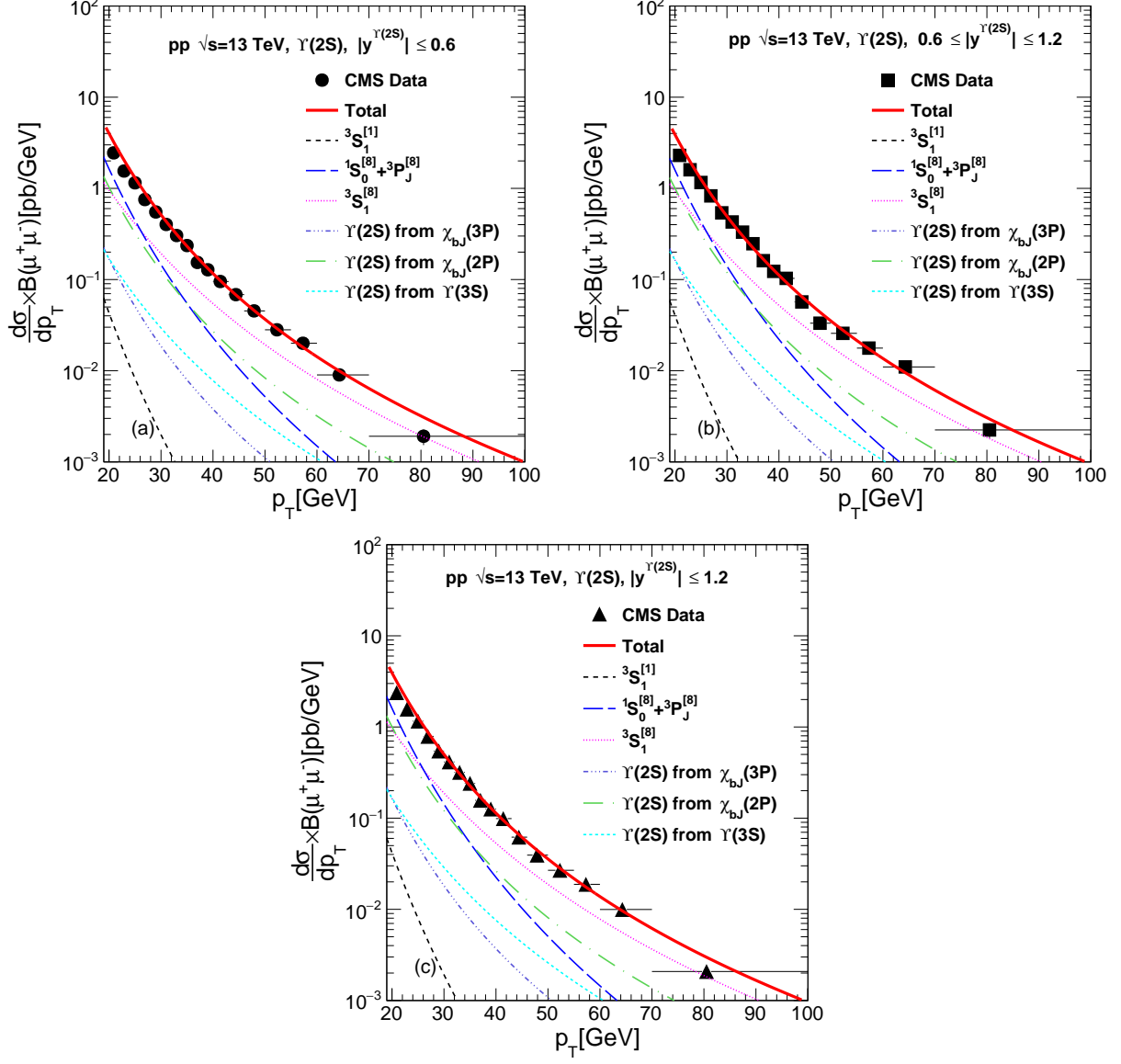


Figure 6: The NRQCD calculations of production cross-section of $\Upsilon(2S)$ in p+p collisions at $\sqrt{s} = 13$ TeV in central and forward rapidities, as a function of transverse momentum compared with the measured data at CMS [35] experiment.

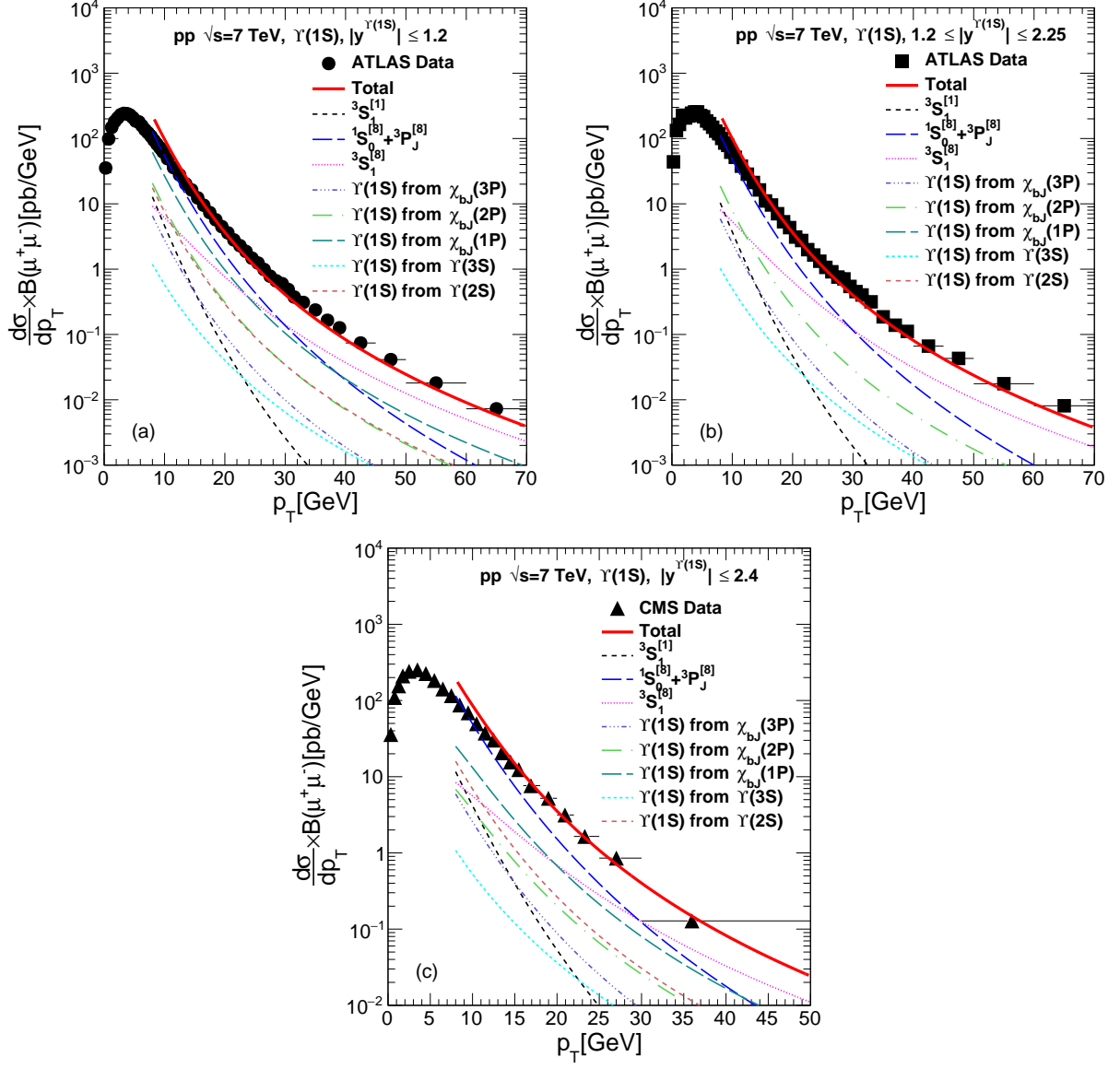


Figure 7: The NRQCD calculations of production cross-section of $\Upsilon(1S)$ in p+p collisions at $\sqrt{s} = 7$ TeV in central and forward rapidities, as a function of transverse momentum compared with the measured data at ATLAS [33] and CMS [34] experiments.

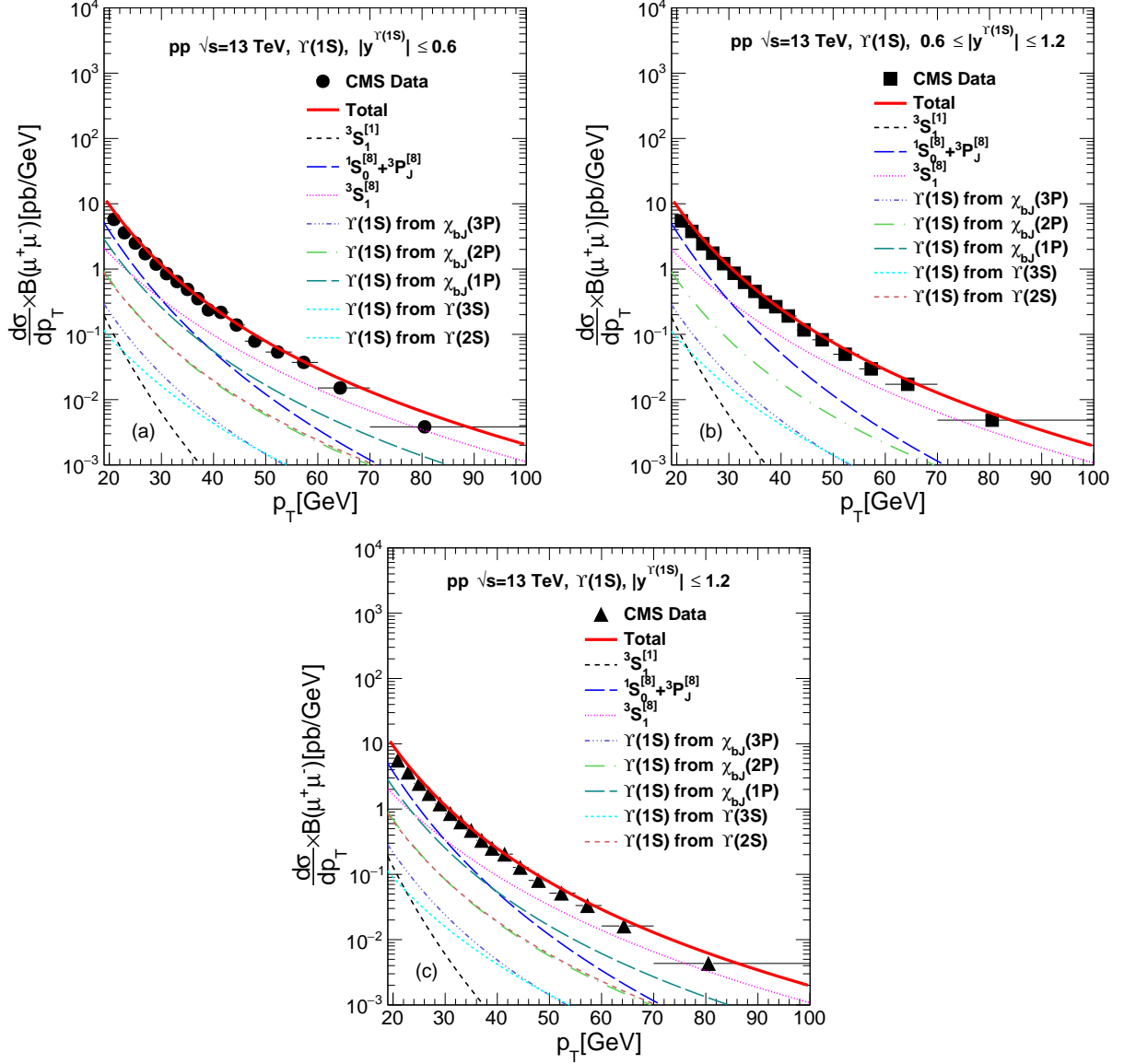


Figure 8: The NRQCD calculations of production cross-section of $\Upsilon(1S)$ in p+p collisions at $\sqrt{s} = 13$ TeV in central and forward rapidities, as a function of transverse momentum compared with the measured data at CMS [35] experiment.

PDFs. In each case however, they have extracted either of the two parameters considering the other to be vanishing. The work in Ref. [21] concentrates only on S-wave colour states. In Refs. [24, 25], the parameters, $M_L([^1S_0]_8)$ and $\frac{M_L([^3P_0]_8)}{m_b^2}$ have been extracted separately altogether. On the other hand in Ref. [26], the authors have considered different combinations of colour octet states to fit with the experimental data with NRQCD at LO and NLO using CTEQ6L1 and CTEQ6M PDFs respectively with $m_b=4.75$ GeV and $[^3S_1]_1=3.54$ GeV³. Their extracted parameters are,

$$\begin{aligned} M_{0,r_0} &= [^1S_0]_8 + \frac{r_0}{m_b^2} [^3P_0]_8 = 0.0283 \pm 0.0007 \text{ GeV}^3 \\ M_{1,r_1} &= [^3S_1]_8 + \frac{r_1}{m_b^2} [^3P_0]_8 = 0.0083 \pm 0.0002 \text{ GeV}^3 \end{aligned} \quad (5)$$

with $r_0=3.8$ and $r_1=-0.52$ GeV².

After fixing the $\Upsilon(3S)$ yield, we next consider $\Upsilon(2S)$ production that has feed down contributions from $\Upsilon(3S)$, $\chi_b(3P)$ and $\chi_b(2P)$ states along with the direct production. The corresponding branching fractions for the feed down sectors are given in Table 1. We have used our extracted values of the $\Upsilon(3S)$ LDMEs for the feed down contributions from the $\Upsilon(3S)$. To include the $\chi_b(nP)$ states feed down LDMEs are obtained from Ref. [22, 25].

In Fig 5, we have shown our NRQCD predictions of production cross-sections for $\Upsilon(2S)$ in p+p collisions as functions of p_T along with the measured data in CMS [34] and ATLAS [33] detectors at central and forward rapidities. All the contributions alongwith feed down ones are displayed separately. Fig. 6 describes the same alongwith the data from CMS detector at 13 TeV for both central and forward rapidities. Our results of CO LDMEs for $\Upsilon(2S)$ have been given in Table 4 along with existing results from different other groups. Our value for $M_L(b\bar{b}([^3S_1]_8 \rightarrow \Upsilon(2S)))$ is in agreement with the values from other groups also $M_L(b\bar{b}([^1S_0]_8, [^3P_0]_8 \rightarrow \Upsilon(2S)))$ does not have negative value (which is unphysical) unlike some other groups. The inclusion of 13 TeV data along with the incorporation of feed down from $\chi_b(3P)$, is expected to give better constrains of LDMEs.

In [19, 20, 22, 24, 25, 26], authors have considered different combinations of CO LDMEs that has already been described. In Ref. [26], the extracted parameters for $\Upsilon(2S)$ are,

$$\begin{aligned} M_{0,r_0} &= 0.0607 \pm 0.0108 \text{ GeV}^3 \\ M_{1,r_1} &= 0.0108 \pm 0.0020 \text{ GeV}^3 \end{aligned}$$

with $[^3S_1]_1=4.63$ GeV³ and the values of r_0 and r_1 are same as given before. The χ^2/ndof for the combined fit in our analysis is ~ 3 .

Having completed $\Upsilon(3S)$ and $\Upsilon(2S)$ parts, we now move on to explore $\Upsilon(1S)$. Alongwith the direct yield, it has feed down contributions from higher S-wave states like $\Upsilon(3S)$ and $\Upsilon(2S)$, as well as P-wave states like $\chi_b(3P)$, $\chi_b(2P)$ and $\chi_b(1P)$. The associated branching functions are provided in Table 1. The extracted CO-LDMEs for $\Upsilon(3S)$ and $\Upsilon(2S)$ are used for feed down contributions, whereas the LDMEs for the $\chi_b(nP)$ states have been taken from Ref. [22, 25] for this present case study. In Fig. 7, we have displayed our NRQCD calculation of production cross-section of $\Upsilon(1S)$ as function of p_T along with the experimental measurements by ATLAS and CMS at $\sqrt{s}=7$ TeV in central rapidities. Finally in Fig. 8, we present our

Table 4: Comparison of CS elements and CO LDMEs extracted from fitting with experimental data using NRQCD formalism for $\Upsilon(2S)$.

Ref. (LO/NLO)	PDF	m_b (GeV)	$M_L(b\bar{b}([{}^3S_1]_1 \rightarrow \Upsilon(2S))$ (GeV ³)	$M_L(b\bar{b}([{}^3S_1]_8 \rightarrow \Upsilon(2S))$ (GeV ³)	$M_L(b\bar{b}([{}^1S_0]_8, [{}^3P_0]_8 \rightarrow \Upsilon(2S))$ (GeV ³)	p_T -cut GeV/ c
present (LO)	CT14LO	4.88	4.5	0.0400±0.0016±0.0023	0.0405±0.0018±0.0029	8
[19] (LO)	CTEQ4L	4.88	5.01	0.040±0.029	0	2
				0.073±0.018	0	4
				0.103±0.027	0	8
[20] (LO)	CTEQ5L	4.77	5.0±0.7	0.180±0.056	-0.102±0.097	8
				0.172±0.050	-0.106±0.102	
	MRSTLO	4.77	5.0±0.7	0.196±0.063 0.190±0.056	-0.087±0.111 -0.089±0.117	8
[22] (LO)	MSTW08LO	4.88	4.5	0.0224±0.0200	-0.0067±0.0084	-
[24] (NLO)	CTEQ6M	5.01	4.63	0.0030±0.0078	0.0075±0.0217	8
[25] (NLO)	CTEQ6M	5.01	4.63	0.0222±0.0024	-0.0003±0.0203	8

Table 5: Comparison of CS elements and CO LDMEs extracted from fitting with experimental data using NRQCD formalism for $\Upsilon(1S)$.

Ref. (LO/NLO)	PDF	m_b (GeV)	$M_L(b\bar{b}([{}^3S_1]_1 \rightarrow \Upsilon(1S))$ (GeV ³)	$M_L(b\bar{b}([{}^3S_1]_8 \rightarrow \Upsilon(1S))$ (GeV ³)	$M_L(b\bar{b}([{}^1S_0]_8, [{}^3P_0]_8 \rightarrow \Upsilon(1S))$ (GeV ³)	p_T -cut GeV/ c
present (LO)	CT14LO	4.88	10.9	$0.0556 \pm 0.0017 \pm 0.0030$	$0.0735 \pm 0.0016 \pm 0.0060$	8
[19] (LO)	CTEQ4L	4.88	11.1	0.077 ± 0.017	0	2
				0.087 ± 0.016	0	4
				0.106 ± 0.013	0	8
[20] (LO)	CTEQ5L	4.77	12.8 \pm 1.6	0.116 ± 0.027	0.109 ± 0.062	8
				0.124 ± 0.025	0.111 ± 0.065	
	MRSTLO	4.77	12.8 \pm 1.6	0.117 ± 0.030 0.130 ± 0.028	0.181 ± 0.072 0.186 ± 0.075	8
[22] (LO)	MSTW08LO	4.88	10.9	0.0477 ± 0.0334	0.0121 ± 0.0400	-
[24] (NLO)	CTEQ6M	4.75	9.282	-0.0041 ± 0.0024	0.0780 ± 0.0043	8
[25] (NLO)	CTEQ6M	PDG	9.282	0.0061 ± 0.0024	0.0895 ± 0.0248	8

results along with the CMS measurements at 13 TeV with all the components separately to signify their relative contributions.

Table 5 shows our results for $\Upsilon(1S)$ parameters along with the results from different groups. The individual values of LDMEs are in agreement with the values from previous works but with considerable reduction in errors upon inclusion of 13 TeV data sets from CMS. The values of the parameters M_{0,r_0} and M_{1,r_1} extracted in Ref. [26] are,

$$M_{0,r_0} = 0.1370 \pm 0.0111 \text{ GeV}^3,$$

$$M_{1,r_1} = 0.0117 \pm 0.0002 \text{ GeV}^3$$

with $[{}^3S_1]_1=9.28 \text{ GeV}^3$ keeping r_0 and r_1 same as given before.

4. Summary

We have presented NRQCD calculations for the differential production cross-sections of Υ states in p+p collisions. Measured transverse momentum distributions of $\Upsilon(3S)$, $\Upsilon(2S)$ and $\Upsilon(1S)$ in p + \bar{p} collisions at $\sqrt{s} = 1.8 \text{ TeV}$ and in p+p collisions at 7 TeV and 13 TeV are used to constrain the LDMEs. All the relevant feeddown contributions from higher mass states including the $\chi_b(3P)$ are taken in to account. The calculations for $\Upsilon(3S)$, $\Upsilon(2S)$ and $\Upsilon(1S)$ are compared with the measured data at Tevatron and LHC.

The formalism provides very good description of the data in large transverse momentum range at different collision energy. We compare the LDMEs for bottomonia obtained in this analysis with the results from earlier works. At high p_T , the colour singlet contribution is very small and LHC data in large p_T range help to constrain the relative contributions of different colour octet contributions. For Υ states at high p_T , the contribution of the $M_L(b\bar{b}([{}^3S_1]_8 \rightarrow \Upsilon(nS)))$ is highest which is opposite to the charmonia case where the contribution for the combination of $M_L(c\bar{c}([{}^1S_0]_8, [{}^3P_0]_8) \rightarrow \psi)$ is more [36]. In summary, we present a comprehensive lowest-order analysis of hadroproduction data of bottomonia states using the latest parton distribution functions and including very recent LHC data. The feed-down contributions from all the χ_b states are included in the calculations. The values of relevant LDMEs are extracted by doing a simultaneous fit of all the data sets. These values will be useful for predictions of quarkonia cross-section and for the purpose of a comparison with those obtained using the NLO formulations.

acknowledgement

Authors thank Board of Research in Nuclear Sciences (BRNS) and UGC (DRS) for support. AB thanks Alexander von Humboldt (AvH) foundation and Federal Ministry of Education and Research (Germany) for support through Research Group Linkage Programme. KS acknowledges the financial support from DST-SERB under NPDF file no. PDF/2017/002399.

References

References

- [1] B. Povh, K. Rith, C. Scholz, F. Zersche and W. Rodejohann, “Particles and nuclei: An Introduction to the physical concepts,” 10.1007/978-3-662-46321-5
- [2] S. M. Ikhdaire and R. Sever, “A Systematic study on nonrelativistic quarkonium interaction,” *Int. J. Mod. Phys. A* **21** (2006), 3989 [arXiv:hep-ph/0508144 [hep-ph]].
- [3] A. M. Sirunyan *et al.* [CMS Collaboration], “Measurement of prompt and nonprompt charmonium suppression in PbPb collisions at 5.02 TeV,” *Eur. Phys. J. C* **78** (2018) 509.
- [4] A. M. Sirunyan *et al.* [CMS Collaboration], “Measurement of nuclear modification factors of $\Upsilon(1S)$, $\Upsilon(2S)$, and $\Upsilon(3S)$ mesons in PbPb collisions at $\sqrt{s_{NN}} = 5.02$ TeV,” *Phys. Lett. B* **790** (2019) 27.
- [5] S. Acharya *et al.* [ALICE Collaboration], “Studies of J/ψ production at forward rapidity in PbPb collisions at $\sqrt{s_{NN}} = 5.02$ TeV,” *JHEP* **2002** (2020) 041.
- [6] S. Acharya *et al.* [ALICE Collaboration], “ Υ suppression at forward rapidity in PbPb collisions at $\sqrt{s_{NN}} = 5.02$ TeV,” *Phys. Lett. B* **790** (2019) 89.
- [7] M. Strickland, “Thermal $\Upsilon(1S)$ and χ_{b1} suppression in $\sqrt{s_{NN}} = 2.76$ TeV PbPb collisions at the LHC,” *Phys. Rev. Lett.* **107** (2011) 132301 [arXiv:1106.2571 [hep-ph]].

- [8] T. Song, K. C. Han and C. M. Ko, “Bottomonia suppression in heavy-ion collisions,” *Phys. Rev. C* **85** (2012) 014902 [arXiv:1109.6691 [nucl-th]].
- [9] V. Kumar, P. Shukla and R. Vogt, “Quarkonia suppression in PbPb collisions at $\sqrt{s_{NN}} = 2.76$ TeV,” *Phys. Rev. C* **92** (2015) 024908 [arXiv:1410.3299 [hep-ph]].
- [10] V. Kumar, P. Shukla and A. Bhattacharyya, “Suppression of quarkonia in PbPb collisions at $\sqrt{s_{NN}} = 5.02$ TeV,” *J. Phys. G* **47**, (2020) 015104.
- [11] P. Nason, S. Dawson and R. K. Ellis, “The One Particle Inclusive Differential Cross-Section for Heavy Quark Production in Hadronic Collisions,” *Nucl. Phys. B* **327** (1989) 49 Erratum: [*Nucl. Phys. B* **335** (1990) 260].
- [12] G. T. Bodwin, E. Braaten and G. P. Lepage, “Rigorous QCD analysis of inclusive annihilation and production of heavy quarkonium,” *Phys. Rev. D* **51** (1995) 1125 Erratum: [*Phys. Rev. D* **55** (1997) 5853]
- [13] N. Brambilla *et al.*, “QCD and Strongly Coupled Gauge Theories: Challenges and Perspectives,” *Eur. Phys. J. C* **74** (2014) 2981
- [14] M. B. Einhorn and S. D. Ellis, “Hadronic Production of the New Resonances: Probing Gluon Distributions,” *Phys. Rev. D* **12** (1975) 2007.
- [15] E. L. Berger and D. L. Jones, “Inelastic Photoproduction of J/psi and Upsilon by Gluons,” *Phys. Rev. D* **23** (1981) 1521.
- [16] H. Fritzsch, “Producing Heavy Quark Flavors in Hadronic Collisions: A Test of Quantum Chromodynamics,” *Phys. Lett.* **67B** (1977) 217.
- [17] J. F. Amundson, O. J. P. Eboli, E. M. Gregores and F. Halzen, “Colorless states in perturbative QCD: Charmonium and rapidity gaps,” *Phys. Lett. B* **372** (1996) 127 [hep-ph/9512248].
- [18] J. L. Domenech and M. A. Sanchis-Lozano, “Bottomonium production at the Tevatron and the LHC,” *Phys. Lett. B* **476** (2000) 65 [hep-ph/9911332].
- [19] J. L. Domenech and M. A. Sanchis-Lozano, “Results from bottomonia production at the Tevatron and prospects for the LHC,” *Nucl. Phys. B* **601** (2001) 395 [hep-ph/0012296].
- [20] E. Braaten, S. Fleming and A. K. Leibovich, “NRQCD analysis of bottomonium production at the Tevatron,” *Phys. Rev. D* **63** (2001) 094006 [hep-ph/0008091].
- [21] B. Gong, J. X. Wang and H. F. Zhang, “QCD corrections to Υ production via color-octet states at the Tevatron and LHC,” *Phys. Rev. D* **83** (2011) 114021 [arXiv:1009.3839 [hep-ph]].
- [22] R. Sharma and I. Vitev, “High transverse momentum quarkonium production and dissociation in heavy ion collisions,” *Phys. Rev. C* **87**, 044905 (2013).

- [23] P. Sun, C.-P. Yuan and F. Yuan, “Heavy Quarkonium Production at Low Pt in NRQCD with Soft Gluon Resummation,” *Phys. Rev. D* **88** (2013) 054008 [arXiv:1210.3432 [hep-ph]].
- [24] B. Gong, L. P. Wan, J. X. Wang and H. F. Zhang, “Complete next-to-leading-order study on the yield and polarization of $\Upsilon(1S, 2S, 3S)$ at the Tevatron and LHC,” *Phys. Rev. Lett.* **112** (2014), 032001 [arXiv:1305.0748 [hep-ph]].
- [25] Y. Feng, B. Gong, L. P. Wan and J. X. Wang, “An updated study of Υ production and polarization at the Tevatron and LHC,” *Chin. Phys. C* **39** (2015) 123102 [arXiv:1503.08439 [hep-ph]].
- [26] H. Han, Y. Q. Ma, C. Meng, H. S. Shao, Y. J. Zhang and K. T. Chao, “ $\Upsilon(nS)$ and $\chi_b(nP)$ production at hadron colliders in nonrelativistic QCD,” *Phys. Rev. D* **94** (2016), 014028 [arXiv:1410.8537 [hep-ph]].
- [27] Y. Feng, B. Gong, C. H. Chang and J. X. Wang, “Complete study on polarization of $\Upsilon(nS)$ hadroproduction at QCD next-to-leading order,” *Chin. Phys. C* **45** (2021) 013117, [arXiv:2009.03028 [hep-ph]].
- [28] G. M. Yu, Y. B. Cai, Y. D. Li and J. S. Wang, “Heavy quarkonium photoproduction in ultrarelativistic heavy ion collisions,” *Phys. Rev. C* **95** (2017) 014905 Addendum: [*Phys. Rev. C* **95** (2017) 069901] [arXiv:1703.03194 [hep-ph]].
- [29] B. Gong and J. X. Wang, “QCD corrections to polarization of J/ψ and Υ at Tevatron and LHC,” *Phys. Rev. D* **78** (2008), 074011 [arXiv:0805.2469 [hep-ph]].
- [30] D. Acosta *et al.* [CDF Collaboration], “ Υ Production and Polarization in $p\bar{p}$ Collisions at $\sqrt{s} = 1.8$ TeV,” *Phys. Rev. Lett.* **88** (2002) 161802.
- [31] R. Aaij *et al.* [LHCb Collaboration], “Measurement of Upsilon production in pp collisions at $\sqrt{s} = 7$ TeV,” *Eur. Phys. J. C* **72** (2012) 2025, [arXiv:1202.6579 [hep-ex]].
- [32] V. Khachatryan *et al.* [CMS Collaboration], “Measurements of the $\Upsilon(1S)$, $\Upsilon(2S)$, and $\Upsilon(3S)$ differential cross sections in pp collisions at $\sqrt{s} = 7$ TeV,” *Phys. Lett. B* **749**, (2015), 14. [arXiv:1501.07750 [hep-ex]].
- [33] G. Aad *et al.* [ATLAS Collaboration], “Measurement of Upsilon production in 7 TeV pp collisions at ATLAS,” *Phys. Rev. D* **87** (2013) 052004, [arXiv:1211.7255 [hep-ex]].
- [34] S. Chatrchyan *et al.* [CMS Collaboration], “Measurement of the $\Upsilon(1S)$, $\Upsilon(2S)$, and $\Upsilon(3S)$ Cross Sections in pp Collisions at $\sqrt{s} = 7$ TeV,” *Phys. Lett. B* **727** (2013) 101, [arXiv:1303.5900 [hep-ex]].
- [35] A. M. Sirunyan *et al.* [CMS Collaboration], “Measurement of quarkonium production cross sections in pp collisions at $\sqrt{s} = 13$ TeV,” *Phys. Lett. B* **780** (2018) 251, [arXiv:1710.11002 [hep-ex]].
- [36] V. Kumar and P. Shukla, “Charmonia production in p+p collisions under NRQCD formalism,” *J. Phys. G* **44**, (2017) 085003.

- [37] R. Baier and R. Ruckl, “Hadronic Collisions: A Quarkonium Factory,” *Z. Phys. C* **19**, (1983) 251.
- [38] B. Humpert, “Narrow Heavy Resonance Production By Gluons,” *Phys. Lett. B* **184**, (1987) 105.
- [39] R. Gastmans, W. Troost and T. T. Wu, “Production of Heavy Quarkonia From Gluons,” *Nucl. Phys. B* **291**, (1987) 731.
- [40] P. L. Cho and A. K. Leibovich, “Color octet quarkonia production,” *Phys. Rev. D* **53**, (1996) 150.
- [41] P. L. Cho and A. K. Leibovich, “Color octet quarkonia production. 2.,” *Phys. Rev. D* **53** (1996), 6203.
- [42] P. A. Zyla *et al.* [Particle Data Group], “Review of Particle Physics,” *PTEP* **2020** (2020) 083C01.
- [43] T. J. Hou, J. Gao, T. J. Hobbs, K. Xie, S. Dulat, M. Guzzi, J. Huston, P. Nadolsky, J. Pumplin and C. Schmidt, *et al.* “New CTEQ global analysis of quantum chromodynamics with high-precision data from the LHC,” *Phys. Rev. D* **103** (2021), 014013.